




# Analysis of the interactions in FCCF:(H<sub>2</sub>O) and FCCF:(H<sub>2</sub>O)<sub>2</sub> complexes through the study of their indirect spin–spin coupling constants

María Cristina Caputo, Ibon Alkorta, Patricio F. Provasi & Stephan P. A. Sauer



To cite this article: María Cristina Caputo, Ibon Alkorta, Patricio F. Provasi & Stephan P. A. Sauer (2018): Analysis of the interactions in FCCF:(H<sub>2</sub>O) and FCCF:(H<sub>2</sub>O)<sub>2</sub> complexes through the study of their indirect spin–spin coupling constants, Molecular Physics, DOI: [10.1080/00268976.2018.1488006](https://doi.org/10.1080/00268976.2018.1488006)

To link to this article: <https://doi.org/10.1080/00268976.2018.1488006>

 View supplementary material 

 Published online: 22 Jun 2018.

 Submit your article to this journal 

 View related articles 

 View Crossmark data 

# Analysis of the interactions in FCCF:(H<sub>2</sub>O) and FCCF:(H<sub>2</sub>O)<sub>2</sub> complexes through the study of their indirect spin–spin coupling constants

María Cristina Caputo<sup>a</sup>, Ibon Alkorta <sup>b</sup>, Patricio F. Provasi<sup>c</sup> and Stephan P. A. Sauer <sup>d</sup>

<sup>a</sup>Departamento de Física, Facultad de Ciencias Exactas y Naturales, Universidad de Buenos Aires y IFIBA – CONICET-UBA, Ciudad Universitaria, Buenos Aires, Argentina; <sup>b</sup>Instituto de Química Médica (C.S.I.C.), Madrid, Spain; <sup>c</sup>Department of Physics – IMIT – CONICET, Northeastern University, Corrientes, Argentina; <sup>d</sup>Department of Chemistry, University of Copenhagen, Copenhagen Ø, Denmark

## ABSTRACT

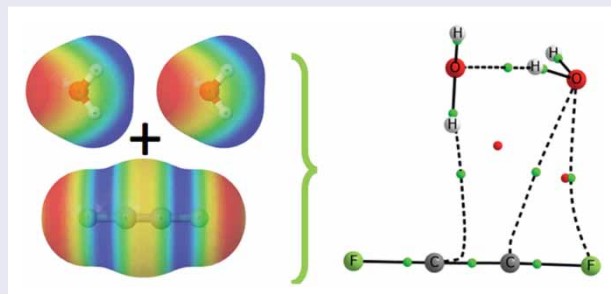
A theoretical study of FCCF:(H<sub>2</sub>O)<sub>n</sub> complexes, with  $n = 1$  and 2, has been carried out by means of ab initio computational methods. Three kinds of interactions are observed in the complexes: H... $\pi$  and H...F hydrogen bonds and O...FC tetrel bonds. The indirect spin–spin coupling constants have been calculated at the CCSD/aug-cc-pVTZ-J computational level. Special attention has been paid to the dependence of the different intramolecular coupling constants in FCCF on the distance between the coupled nuclei and the presence or absence of water molecules. The exceptional sensitivity shown by these coupling constants to the presence of water molecules is quite notorious and can provide information on the bonding structure of the molecule.

## ARTICLE HISTORY

Received 20 April 2018  
Accepted 31 May 2018

## KEYWORDS

Spin–spin coupling constants; difluoroacetylene; weak interaction; tetrel bond; hydrogen bond



## 1. Introduction

Nuclear magnetic resonance (NMR) spectroscopy is one of the branches of spectroscopy most developed in the last years, and it is crucial in the investigation of the structure of molecules and their conformation. Particularly, the indirect NMR spin–spin coupling constants (SSCCs) provide valuable insight into the bonding situation of a molecule [1–10].

According to the classic theory of Ramsey [11], there are four different contributions, the diamagnetic spin–orbit (DSO) term, the paramagnetic spin–orbit (PSO) term, the Fermi contact (FC) term and the spin–dipole (SD) term, which add to the indirect isotropic SSCC. Each of these terms probes the electron density of a molecule in a different way.

DSO and PSO terms arise from the orbital currents induced by the nuclei magnetic fields; the FC term is mediated by the spin polarisation of the contact density at the nuclei while the SD term results from the spin polarisation caused by the magnetic dipole field of the nuclear moments. Accordingly, the FC term depends preferentially on the  $\sigma$ -electrons of a molecule because only those possess a substantial density value at the contact surface of the nucleus. The DSO term is large at positions of high spin density, but otherwise, its magnitude is mostly smaller than that of the PSO term. The latter as well as the SD term is sensitive to the presence of  $\pi$ -electrons.

Considering the normally small magnitude of the DSO term, one can simplify these observations by stating

that the FC term probes the  $\sigma$ -electronic structure of a molecule while the non-contact (NC) terms probe its  $\pi$ -electronic structure [12]. This could be used to determine via the SSCC and its four Ramsey terms the  $\pi$ -character of a bond.

The study of the intramolecular SSCCs for hydrogen bonded complexes of difluoroethyne is interesting because of their large value and their well-known sensitivity to charges induced in the electronic cloud like those caused by hydrogen bonding [13].

The indirect SSCCs in difluoroethyne (difluoroacetylene), FCCF, have been a challenging test for computational methods. The experimental values, described by Bürger and Sommer [14], are 2.1 Hz for  $^3J(^{19}\text{F}-^{19}\text{F})$  and  $-287.3$  Hz for  $^1J(^{19}\text{F}-^{13}\text{C})$ . Recently, Del Bene *et al.* [15] were able to compute values similar to the experimental ones using the EOM-CCSD/Ahlrichs qzp computational level and the experimental geometry reported by Bürger *et al.* [16]. The computed values were 1.4 Hz for  $^3J(^{19}\text{F}-^{19}\text{F})$ ,  $-277.7$  Hz for  $^1J(^{19}\text{F}-^{13}\text{C})$  and 40.2 Hz for  $^2J(^{19}\text{F}-^{13}\text{C})$ . This last value was also estimated by Del Bene *et al.* from the experimental spectrum to be 28.7 Hz [15]. Sauer and co-workers [17–21] applied the specialised core-property basis sets aug-cc-pVTZ-J and (aug)-ccJ-pVXZ ( $X = \text{D, T, Q, 5}$ ) in combination with SOPPA, SOPPA (CCSD), CCSD, CC3 and even CCSDT levels of theory and optimised geometries to the study of the indirect coupling constants in difluoroethyne. They found that the vibrational effects to  $^3J(^{19}\text{F}-^{19}\text{F})$  are of the same order of magnitude as the equilibrium geometry value of this coupling constant [19], that triples corrections to the one- and three-bond couplings calculated at the CC3 level are in the order of 4–6 Hz [19,20] and that using the aug-ccJ-pVTZ basis set there is still a remaining basis set error compared to the basis set limit of 2–3 Hz [21]. The currently most accurately calculated values of the coupling constants in difluoroethyne are thus 2.56 Hz for  $^3J(^{19}\text{F}-^{19}\text{F})$ ,  $-256.58$  Hz for  $^1J(^{19}\text{F}-^{13}\text{C})$ , 45.14 Hz for  $^2J(^{19}\text{F}-^{13}\text{C})$  and 401.65 Hz for  $^1J(^{13}\text{C}-^{13}\text{C})$  calculated at the CC3/aug-ccJ-pVTZ level at a CCSD(T)/cc-pCVQZ geometry [20].

In two previous articles, we analysed the intramolecular spin–spin coupling constant in HCN and HNC complexes [22] and in particular of FCCF:(HF) $_n$  with  $n = 1$  and 2 [13]. For the latter, we analysed the weight of each of the contributions to the constants,  $^mJ$ , for  $m = 1, 2$  or 3, considering two types of hydrogen bonds: one where the fluorine atoms act as hydrogen bond (HB) acceptors and another where the  $\pi$ -cloud of the  $\text{C}_2\text{F}_2$  moiety is the HB acceptor.

In this paper, we study the changes on the inter- and intra- spin–spin coupled constants brought about by the presence of water molecules around difluoroacetylene

[FCCF:(H $_2$ O) $_n$ ; with  $n = 1, 2$ ]. We have considered the three possible types of complexes, with HOH $\cdots\pi$  interactions, with HOH $\cdots$ FC hydrogen bonds and with O $\cdots$ (FC) tetrel bonds [23,24], with special attention to their dependence on the distance between the coupled nuclei and the location of the bonded water molecules. We also analyse the possible relation of the values of the spin–spin coupled constants to both the bond paths (BP) and bond critical points (BCP) [25].

## 2. Theoretical methods

The geometry of all the systems has been optimised at the MP2 [26] computational level with the 6–311++G(d,p) basis set and the frozen core approximation using the Gaussian-03 program [27]. Frequency calculations have been performed on the minimised geometries in order to confirm that the obtained structures correspond to energetic minima [28].

The many-body interaction-energy formalism (MBIE) has been used to obtain the one-, two- and three-body contributions to the binding energy. The binding energy  $\Delta E$  (Equation (1)) can be decomposed into one- (Equation (2)), two- (Equation (3)), and three-body terms (Equation (4)), as:

$$\Delta E = E(ABC) - \sum_{i=A}^C E_m(i) = \sum_{i=A}^C [E(i) - E_m(i)] + \sum_{i=A}^B \sum_{j>i}^C \Delta^2 E(ij) + \Delta^3 E(ABC), \quad (1)$$

$$E_R(i) = E(i) - E_m(i), \quad (2)$$

$$\Delta^2 E(ij) = E(ij) - [E(i) + E(j)], \quad (3)$$

$$\Delta^3 E(ABC) = E(ABC) - [E(A) + E(B) + E(C)] - [\Delta^2 E(AB) + \Delta^2 E(AC) + \Delta^2 E(BC)], \quad (4)$$

where  $E_m(i)$  corresponds to the energy of the isolated monomer at its equilibrium configuration, and  $E(i)$  to the energy of the monomer with the geometry it has in the complex. The difference between these two energies permits to obtain  $E_R(i)$ , as the monomer distortion energy.  $\Delta^2 E(ij)$  and  $\Delta^3 E(ABC)$  are the two- and three-body interaction energies computed at the corresponding geometries in the complex.

The theory of indirect nuclear SSCCs [11] and the different computational methods used for calculating them have been extensively described in the literature [29–34]. However, it is important to keep in mind that

there are four contributions to the SSCC: the FC and the spin-dipolar (SD) terms, which come from the interaction of the nuclear magnetic moments with the spin of the electrons; the diamagnetic spin orbital (DSO) and the paramagnetic spin orbital (PSO) terms, which are due to the interaction of the nuclear spins with the orbital angular momentum of the electrons.

All coupling constants were calculated at the coupled cluster with single and double excitations (CCSD) level [35–42] using the core-property basis set aug-cc-pVTZ-J basis set [43,44]. This basis set ensures the cusp behaviour of the wave function at the nuclear sites and consequently a very good description of the FC term [43] (and references therein). The CCSD formalism explicitly includes electron correlation effects, which are important for coupling constants involving the more electronegative atoms. In the present work, the calculations were performed using the CFOUR program package [45]. Relativistic corrections [46] can safely be ignored for the molecules in this study but vibrational corrections [47,48] or bulk solvent effects [49,50] should in principle be considered. High-level calculations of vibrational corrections at the CCSD level of theory are still very rare [19,51–53] due to their high cost compared to e.g. SOPPA [54–56] or DFT [57,58] calculations. CCSD calculated vibrational corrections are thus out of the scope for the present study, while adding DFT-calculated vibrational corrections would be inconsistent due to the difference in the optimised geometries. To our knowledge, vibrational corrections to couplings involving fluorine were so far studied only for very few and very small molecules, i.e. HF [57], HFH<sup>−</sup> [59], FCCF [19] and BF<sub>3</sub> [51]. Additional bulk solvent effects could be studied either by a continuum model like PCM [49,60] or the QM/MM approach [50].

### 3. Results and discussions

This section has been divided into four subsections. In the first three ones, the geometry, energy and electronic

properties of the isolated molecules, binary and ternary complexes calculated at MP2/6-311++G(d,p) computational level are discussed, respectively. In the last one, we discussed the inter- and intramolecular coupling constants obtained at CCSD/aug-cc-pVTZ-J level.

#### 3.1. Isolated monomers

The molecular electrostatic potential (MEP) of the FCCF and H<sub>2</sub>O molecules on the 0.001 au electron density isosurface are depicted in Figure 1. The MEP of FCCF shows three characteristic regions, two with negative values of MEP surrounding the F atoms (−0.0055 au) and the  $\pi$ -cloud (−0.0005 au) and a positive region around the C–F bond (+0.0176 au). The water molecule shows positive regions in the extension of the O–H bonds (+0.0708 au) and a negative region associated with the lone pairs (−0.0595 au). Based on these results, three different configurations can be expected based on the complementarity of the MEP of these molecules. On one hand, the positive region associated with the hydrogen atoms of H<sub>2</sub>O could interact with negative regions of the fluorine atoms or the  $\pi$  cloud of the FCCF molecule. On the other hand, the negative region due to the lone pairs of the oxygen in H<sub>2</sub>O could bind to the positive MEP of the C–F bond of FCCF.

#### 3.2. Geometry and energy

##### 3.2.1. Binary complexes

Three minima have been located in the potential energy surface of the FCCF:H<sub>2</sub>O complex (Figure 2 and Table S1 of the Supporting Information), one shows a tetrel bond between the electron deficient C–F bond and the lone pairs of H<sub>2</sub>O (A) and the other two correspond to HBs with the  $\pi$ -cloud of C<sub>2</sub>F<sub>2</sub> (B) or with the F atom (C), in agreement with the MEPs of the two isolated molecules. The first complex (A) is the most stable one (Table 1) with a binding energy of −6.0 kJ/mol followed by B (−4.4 kJ/mol), with C the least stable one (−3.7 kJ/mol).

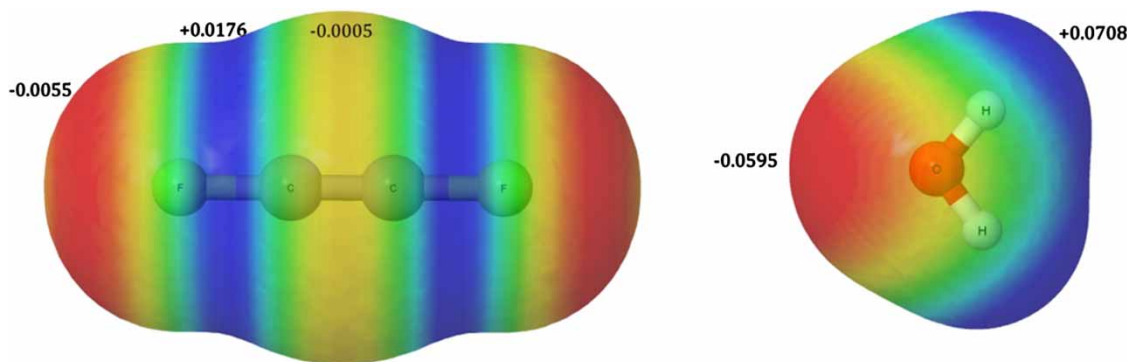


**Figure 1.** Molecular electrostatic potential of the FCCF and H<sub>2</sub>O on the 0.001 au electron density.

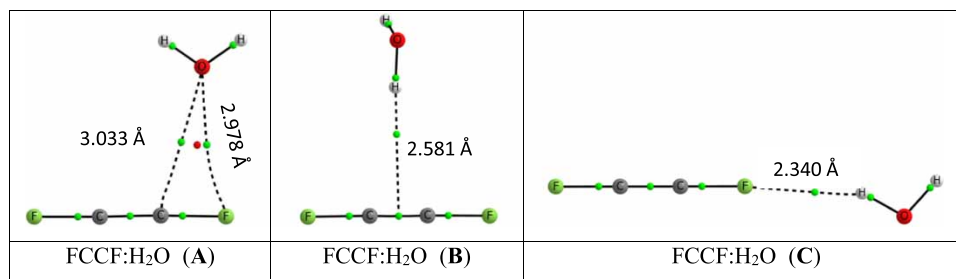


**Figure 2.** Molecular graph of the three minima found for the FCCF:H<sub>2</sub>O complex. The small dots on dashed and solid lines (green in the online version) indicate the location of the bond critical points, while the small dots not superimposed on lines (red in the online version) indicate the location of the ring critical points.

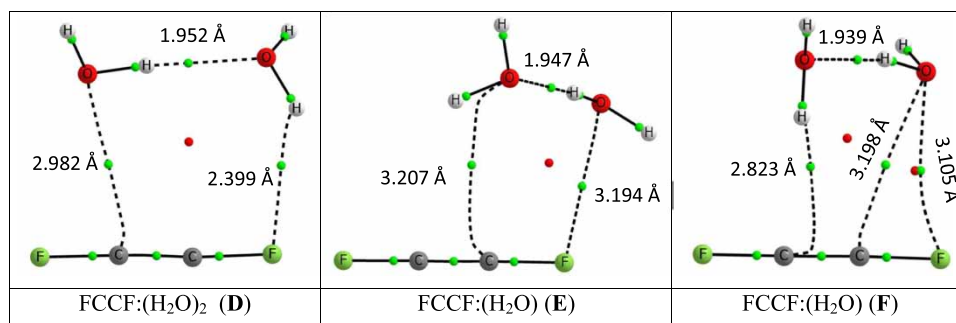


**Figure 3.** Molecular graph of the three minima found for the FCCF:(H<sub>2</sub>O)<sub>2</sub> complex. The small dots on dashed and solid lines (green in the online version) indicate the location of the bond critical points, while the small dots not superimposed on lines (red in the online version) indicate the location of the ring critical points.

Figure 2 shows a single intermolecular bond critical point (BCP) and the corresponding bond path (BP) linking the two groups involved in the HB interactions for complexes (B) and (C), and two BCPs/BPs for the tetrel bonded complex (A) that link the oxygen atom of H<sub>2</sub>O with the C and F atom of FCCF. The characteristics of the BCPs are typical of weak interactions (Table S2 of the supporting information), with  $\rho_{\text{BCP}}$  values between 0.0077 and 0.0063 au and  $\nabla^2\rho_{\text{BCP}}$  between 0.033 and 0.024 au.

### 3.2.2. Ternary complexes

Three unique minima have been located on the FCCF:(H<sub>2</sub>O)<sub>2</sub> potential energy surface (Figure 3 and Table S3). In all cases, the two H<sub>2</sub>O molecules are connected by an HB. It is longer than the one found in the water dimer (1.951 Å) in the case of D (1.952 Å) and slightly shorter in the case E and F (1.947 and 1.939 Å, respectively). In addition, a number of contacts are observed between the water molecules and FCCF. In all the complexes, one O···C bond path is observed. Other contacts are H···F and H··· $\pi$  hydrogen bonds in complexes D and F, respectively, and O···F interactions in complexes E and F. The O···C/F bond path can be ascribed as tetrel bonds.

The binding energy, see Table 1, of the three minima is in a range of only 2 kJ/mol (between −33.4 and −35.6 kJ mol<sup>−1</sup>) being D the most stable one and E

**Table 1.** Total and binding energy FCCF:(H<sub>2</sub>O)<sub>n</sub> ( $n = 0-2$ ) in kJ/mol.

Complex	Electronic energy (Hartree)	Electronic energy (kJ mol <sup>−1</sup> )	Binding energy (kJ mol <sup>−1</sup> )
C <sub>2</sub> F <sub>2</sub>	−275.208076	−722,558.8	
H <sub>2</sub> O	−76.2749205	−200,259.8	
A	−351.485291	−922,824.6	−6.0
B	−351.484691	−922,823.1	−4.4
C	−351.484396	−922,822.3	−3.7
D	−427.771459	−1,123,114.0	−35.6
E	−427.770629	−1,123,111.8	−33.4
F	−427.770620	−1,123,111.8	−33.4

and F the least ones. The MBIE results (Table S4) indicate that the most stabilising two-body term corresponds to the water dimer interaction with energies around −25 kJ mol<sup>−1</sup>. The two-body terms due to the interaction of the water molecules with FCCF range between −3.8 and −5.7 kJ mol<sup>−1</sup>. The three-body term, which is associated with the cooperativity, shows negative values for D and F (−1.2 and −0.6 kJ mol<sup>−1</sup>) and positive for E (0.5 kJ mol<sup>−1</sup>).

The H···O interaction between the two water molecules shows in all the complexes  $\rho_{\text{BCP}}$  values around 0.023 au while in the rest of the interactions  $\rho_{\text{BCP}}$  range between 0.005 and 0.008 au. In all cases, the Laplacian and total energy density show positive values as an indication that they correspond to weak closed shell interactions (Table S2).

**Table 2.** The  $^1J(\text{C}-\text{C})$  (Hz) coupling in  $\text{C}_2\text{F}_2 + n \text{H}_2\text{O}$  ( $n = 0, 1, 2$ ) for the studied complexes.

Complex	$^1J(\text{C}-\text{C})$	$d_{\text{C}-\text{C}}$
$\text{C}_2\text{F}_2$	410.36	1.1973
<b>A</b>	411.50	1.1976
<b>B</b>	405.29	1.1987
<b>C</b>	413.76	1.1970
<b>D</b>	412.80	1.1974
<b>E</b>	409.20	1.1981
<b>F</b>	406.49	1.1988

**Table 3.** The  $^1J(\text{F}-\text{C})$  (Hz) coupling in  $\text{C}_2\text{F}_2$  for the studied complexes.

Complex	$^1J(\text{F}_1-\text{C}_1)$	$d(\text{F}_1-\text{C}_1)$	$^1J(\text{F}_2-\text{C}_2)$	$d(\text{F}_2-\text{C}_2)$
$\text{C}_2\text{F}_2$	-279.46	1.2867	-279.46	1.2867
<b>A</b>	-277.39	1.2839	-272.07	1.2902
<b>B</b>	-287.01	1.2853	-287.01	1.2853
<b>C</b>	-282.52	1.2853	-261.18	1.2890
<b>D</b>	-284.48	1.2805	-255.80	1.2959
<b>E</b>	-281.01	1.2845	-278.56	1.2880
<b>F</b>	-288.99	1.2821	-277.64	1.2891

**Table 4.** The  $^2J(\text{F}-\text{C})$  couplings in  $\text{C}_2\text{F}_2$  for the studied complexes.

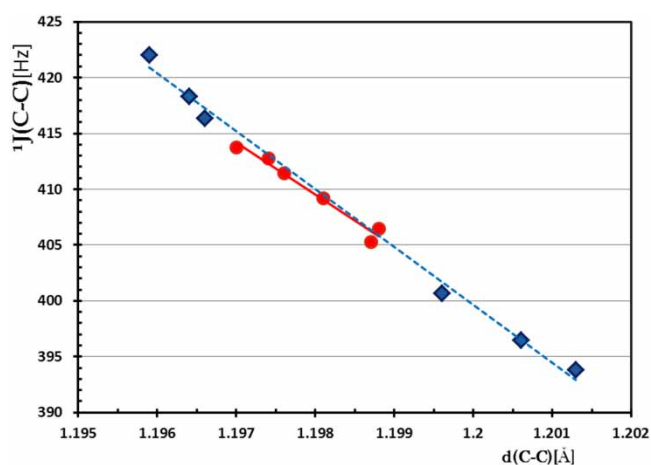
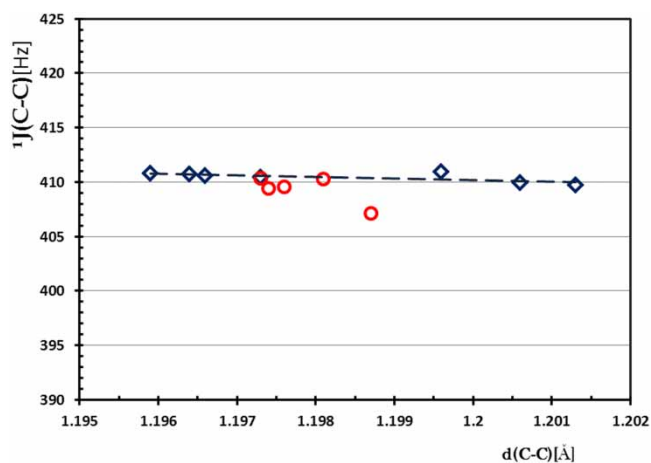
Complex	$d(\text{F}_2-\text{C}_1)$	$^2J(\text{F}_2-\text{C}_1)$	$d(\text{C}-\text{C})$	$^2J(\text{F}_1-\text{C}_2)$	$d(\text{F}_1-\text{C}_2)$
$\text{C}_2\text{F}_2$	2.4840	42.10	1.1973	42.10	2.4840
<b>A</b>	2.4810	42.19	1.1976	42.30	2.4876
<b>B</b>	2.4839	39.89	1.1987	39.89	2.4839
<b>C</b>	2.4822	45.05	1.1969	43.05	2.4859
<b>D</b>	2.4772	42.03	1.1974	44.10	2.4919
<b>E</b>	2.4826	41.32	1.1981	40.88	2.4860
<b>F</b>	2.4806	40.25	1.1988	40.25	2.4877

**Table 5.** The  $^3J(\text{F}-\text{F})$  coupling in  $\text{C}_2\text{F}_2$  for the studied complexes.

Complex	DSO	PSO	SD	FC	Total	$d(\text{F}-\text{F})$
$\text{C}_2\text{F}_2$	-1.8	-39.45	29.81	7.40	-4.04	3.7707
<b>A</b>	-1.74	-39.84	28.94	6.85	-5.79	3.7717
<b>B</b>	-1.76	-39.54	30.75	7.74	-2.81	3.7693
<b>C</b>	-1.75	-39.13	29.07	6.85	-4.96	3.7713
<b>D</b>	-1.68	-40.78	27.91	6.47	-8.09	3.7738
<b>F</b>	-1.7	-39.81	29.61	7.14	-4.75	3.7706
<b>G</b>	-1.7	-39.79	30.22	7.40	-3.88	3.7700

### 3.3. Indirect nuclear SSCCs

The presentation of the analysis of the SSCCs has been divided into two sections, intramolecular and intermolecular couplings. The values of the total coupling constants and the relevant geometrical parameters for the first section are summarised in Tables 2–5 and Figures 4–10, corresponding to the one-, two- and three-bond coupling cases. The results for the intermolecular couplings are depicted in Table 6 and Figure 11. The separate values of the four contributions to the coupling constants are specified in Tables E2 to E6 in the supplementary material. For clarity, we keep the same numbering as in main text. Thus, for instance, Table E4 in the Supplementary Material expands the information of Table 4 in the body of the article.

**Figure 4.** The  $^1J(\text{C}-\text{C})$  (Hz) indirect coupling constant vs. the  $\text{C}\equiv\text{C}$  [Å] bond distance in two different series:  $\blacklozenge$  FCCF:(HF) $_n$  complexes and  $\bullet$  FCCF:(H $_2$ O) $_n$  complexes (this work).**Figure 5.** The  $^1J(\text{C}-\text{C})$  (Hz) indirect coupling constant vs. the  $\text{C}\equiv\text{C}$  [Å] bond distance for isolated  $\text{C}_2\text{F}_2$  in two different cases:  $\blacklozenge$  FCCF with geometry of the FCCF:(FH) $_n$  complexes and  $\circ$  FCCF with geometry of the FCCF:(H $_2$ O) $_n$  complexes (this work).

#### 3.3.1. Intramolecular $^1J(\text{C}-\text{C})$ couplings

The total values of the  $^1J(\text{C}-\text{C})$  couplings and the interatomic C–C distances for all of the studied compounds are summarised in Table 2 (the four contributions are given in Table 2 of the supplementary material). The  $^1J(\text{C}-\text{C})$  values range from 405 to 413 Hz and are completely dominated by the FC term. The contribution of the other three terms (DSO, PSO and SD) is almost constant and thus a perfect linear correlation is obtained between the total  $^1J(\text{C}-\text{C})$  values and the corresponding FC terms ( $R^2 = 0.999$ ).

Figure 4 illustrates the  $^1J(\text{C}-\text{C})$  coupling constants as a function of the length of the  $\text{C}\equiv\text{C}$  bond. We observe that larger values of  $^1J(\text{C}-\text{C})$  are associated with the shorter C–C distances while smaller values are present in the

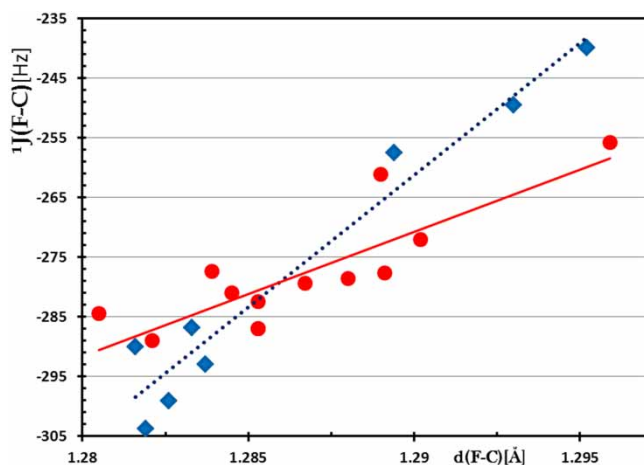


**Figure 6.** The  $^1J(\text{F}-\text{C})$  (Hz) indirect coupling constant vs. the F–C (Å) bond distance in two different series:  $\blacklozenge$  FCCF:(FH) $_n$  complexes and  $\bullet$  FCCF:(H $_2$ O) $_n$  complexes (this work), together with their best trend-lines.

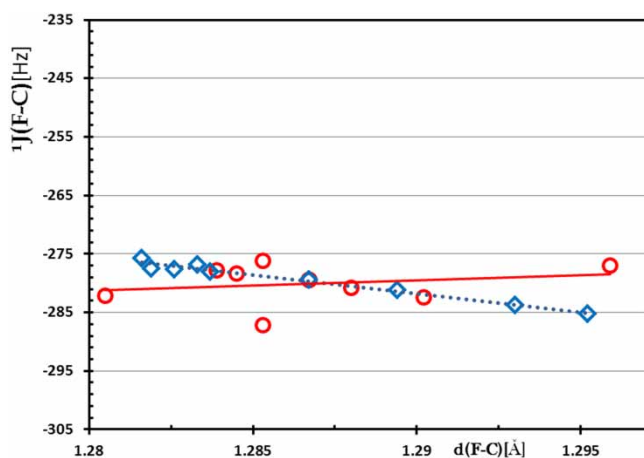


**Figure 7.** The  $^1J(\text{F}-\text{C})$  (Hz) indirect coupling constant vs. the F–C (Å) bond distance for isolated  $\text{C}_2\text{F}_2$  in two different cases: Open circles (squares) correspond to isolated  $\text{C}_2\text{F}_2$  molecules with the geometries they present FCCF:(H $_2$ O) $_n$  [FCCF:(FH) $_n$ ] complexes, together with their best trend lines.

complexes with the longer C–C distances. The range of values of the  $^1J(\text{C}-\text{C})$  coupling constants in the isolated  $\text{C}_2\text{F}_2$  molecule with the geometries of the complexes, Figure 5, is smaller than those in the complexes as indication of the influence of the HB formation on this coupling constant (all the contributions are given in Table 2 of the supplementary material).

Our previous analysis [13] of the interactions between  $\text{C}_2\text{F}_2$  and one or two hydrogen fluoride molecules showed that a 0.1% change in  $d_{\text{C}\equiv\text{C}}$  brings about a 3% difference in  $^1J(\text{C}-\text{C})$ . In this work, see Figure 4, the effect is found to be of the same order, but slightly weaker. Figure 5 shows that it is the nature of the environment and not the change in the  $\text{F}_2\text{C}_2$  geometry, that affects the

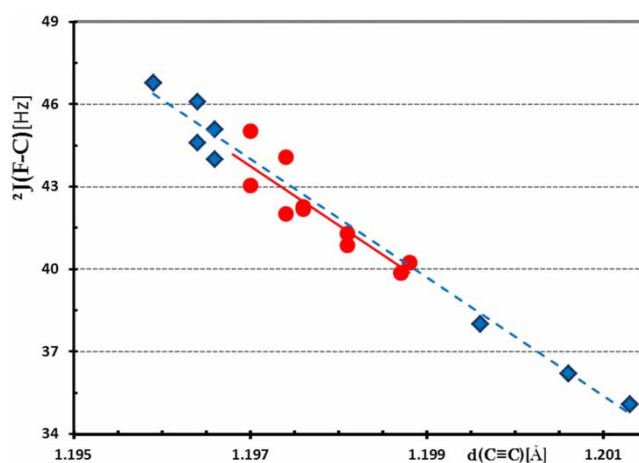


**Figure 8.** The dependence of the  $^2J(\text{F}-\text{C})$  coupling constant on the  $\text{C}\equiv\text{C}$  distance for  $\text{C}_2\text{F}_2$  in complexes with  $\text{H}_2\text{O}$  or HF. The results for FCCF:(H $_2$ O) $_n$  (this work) are shown in solid circles and the solid diamonds show the result for FCCF:(FH) $_n$  complexes.

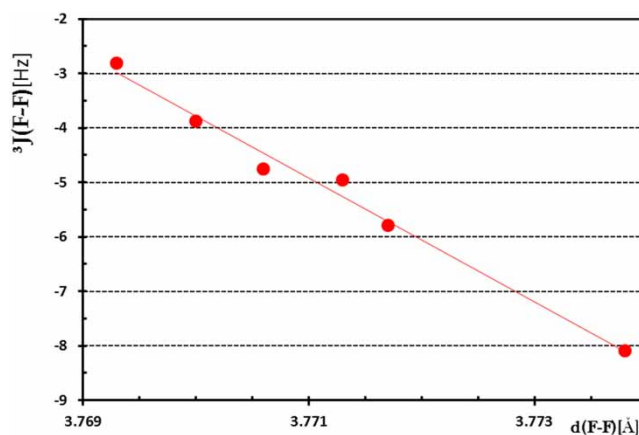


**Figure 9.**  $^3J(\text{F}_2-\text{F}_1)$  indirect coupling constant vs. the F–F bond distance in the studied complexes, the global dependence is illustrated by the straight line.

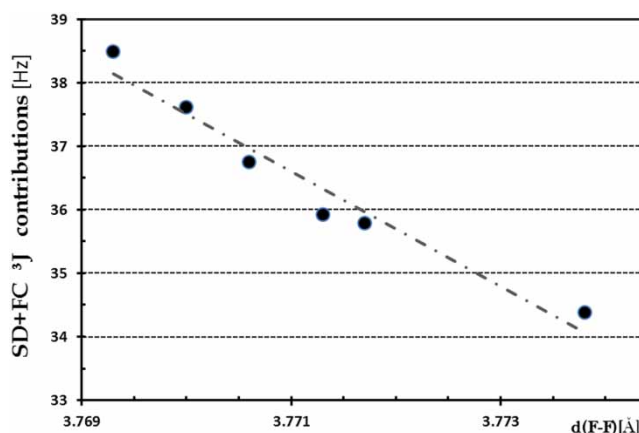


**Figure 10.** The SD + FC contribution  $^3J(\text{F}_2-\text{F}_1)$  vs. the F–F bond distance, the global dependence is illustrated by the dashed straight line.

**Table 6.**  ${}^{n\text{h}}J$  intermolecular indirect coupling constant between  $\text{C}_2\text{F}_2$  and  $\text{H}_2\text{O}$ , with absolute values large than 1.0 Hz, with  $n = 1, 2, t$  (tetrel).

Complex	${}^{1\text{h}}J(\text{F}_i\text{-H}_j)$	$d(\text{F}_i\text{-H}_j)$	${}^xJ(\text{F}_i\text{-O}_j)^{\text{a}}$	$d(\text{F}_i\text{-O}_j)$
<b>A</b>			-8.38 (t)	2.98
<b>C</b>	-4.44	2.34		
<b>D</b>	-2.41	2.40	-6.25 (t) 1.18 (2 h)	3.06 3.18
<b>E</b>			-1.63 (t)	3.24
			1.06 (2 h)	3.19
<b>F</b>			-5.40 (t)	3.10

<sup>a</sup>The nature of the  $x$  interaction is indicated in parenthesis.

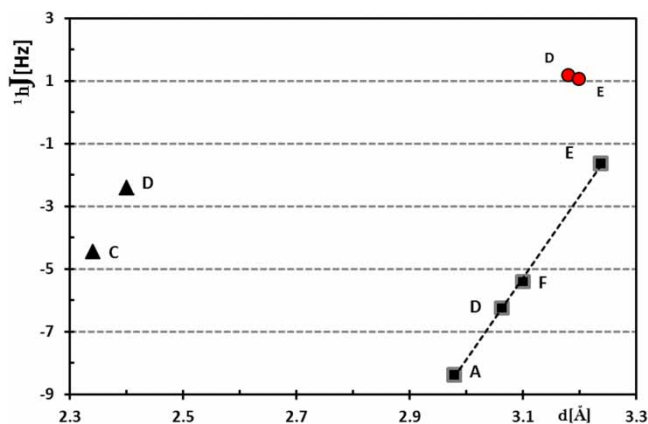


**Figure 11.** The intermolecular  ${}^{1n}J$  between the fluorine nucleus in  $\text{C}_2\text{F}_2$  and one of the nuclei of  $\text{H}_2\text{O}$ . Solid squares depicted  ${}^1J(\text{F}_i\text{-O}_j)$  vs.  $d(\text{F}_i\text{-O}_j)$ , triangles  ${}^{1\text{h}}J(\text{F}_i\text{-H}_j)$  vs.  $d(\text{F}_i\text{-H}_j)$  and circles  ${}^{2\text{h}}J(\text{F}_i\text{-O}_j)$  vs.  $d(\text{F}_i\text{-O}_j)$ .

value of the coupling. In effect, the SSCC results for the isolated FCCF molecule but calculated using the geometry it displays in the complexes, show that the dependence with  $d_{\text{C}\equiv\text{C}}$  is much weaker.

### 3.3.2. Intramolecular ${}^1J(\text{F-C})$ couplings

The results for the  ${}^1J(\text{F-C})$  couplings are summarised in Table 3 (the four contributions are given in Table 3 of the supplementary material). Here, the coupling constants are large and negative in contradiction of the Dirac vector model that predicts positive values for  ${}^1J$ , and in agreement with previous analyses that have reported similar discrepancies [13,61,62].

The FC term is the dominant contribution, as in the  ${}^1J(\text{C-C})$  case (see Table 3 of the supplementary material). The DSO and SD contributions are similar for all the complexes. However, this is not the case of the PSO term that varies between  $-1.3$  and  $-15.5$  Hz. The overall result is that the  ${}^1J(\text{C-F})$  covers a 30 Hz range (between  $-289$  and  $-256$  Hz) while the FC term varies over 21 Hz. (between  $-247$  and  $-268$  Hz). In addition, the linear correlation coefficient, between the total  ${}^1J(\text{F-C})$  values and the corresponding FC terms ( $R^2 = 0.83$ ), is smaller

than in the  ${}^1J(\text{C-C})$  case. The dependence of the  ${}^1J(\text{F-C})$  coupling with the F-C bonding distance is displayed in Figure 6, where the solid circles correspond to the  $\text{C}_2\text{F}_2:n\text{H}_2\text{O}$  complexes. The absolute value of the coupling constant is observed to decrease as the interatomic distance becomes larger. This behaviour, however, cannot be attributed to a mere dependence on the  $\text{C}_2\text{F}_2$  geometry. The results for the  ${}^1J(\text{F-C})$  couplings in isolated  $\text{C}_2\text{F}_2$  molecules, where the molecular geometry is fixed to the one present in the complexes, indicate in fact that in this case the coupling slightly increases in absolute value with the C-F distance. This is illustrated by the open circles in Figure 7.

The differences between the two  ${}^1J(\text{F-C})$  couplings in the same complex is largest for complexes C and D. This corresponds to the two cases that form an HB with the F atom, the larger  ${}^1J$  being associated with the CF moiety involved in the HB interaction, a pattern that had already been observed in  $\text{C}_2\text{F}_2:(\text{HF})_n$  complexes (depicted by solid diamonds in Figure 6). The case of C is particularly conspicuous with larger differences between the  ${}^1J(\text{F-C})$  coupling and the value predicted by trending line. This could be due to C being the only complex with a direct  $\text{F}\cdots\text{H}$  HB in the direction of the F lone pair, which also yields the shortest intermolecular bond in all the studied complexes.

The global dependence of the  ${}^1J(\text{F-C})$  coupling on the FC bond distance is illustrated in Figure 6, showing in solid and dashed style the best trend-lines, respectively, for  $\text{FCCF}:(\text{H}_2\text{O})_n$  and  $\text{FCCF}:(\text{FH})_n$ . Figure 7 is similar, but corresponding to the isolated  $\text{C}_2\text{F}_2$  molecule using the geometries displayed in the complexes.

### 3.3.3. Intramolecular ${}^2J(\text{F-C})$ couplings

The  ${}^2J(\text{F-C})$  couplings are given in Table 4, together with relevant interatomic distances in  $\text{C}_2\text{F}_2$ . The values are positive, again in disagreement with the Dirac vector model. In fact, the three main contributions, PSO, SD and FC, are all positive, with the last one dominating the variations between compounds. No clear dependency of  ${}^2J$  on the corresponding distance  $d(\text{C-F})$  is observed. In fact, basically the same values are obtained for the two couplings in complexes A, E and F, in spite of their different C-F bond lengths. A similar pattern is observed for complex D, where the difference in C-F distance between the two moieties is largest, for only a modest change in the  ${}^2J(\text{F-C})$  coupling constant. This lack of a systematic relation between  ${}^2J$  and  $d(\text{C-F})$  is also illustrated by comparing the results for complexes C and D. The larger of the two  ${}^2J(\text{F-C})$  values corresponds to the shorter CCF distances for complex C, while to the longer CCF distances for the case of complex D. Furthermore for



complex **F**, the two  ${}^2J(\text{F}-\text{C})$  results are identical even though the two CCF distances differ significantly. It is interesting to point out, however, that a systematic relation appears between  ${}^2J$  and  $d(\text{C}\equiv\text{C})$ , as illustrated in Figure 8.

### 3.3.4. Intramolecular ${}^3J(\text{F}-\text{F})$ couplings

The  ${}^3J(\text{F}-\text{F})$  couplings are gathered in Table 5 and plotted as a function of the F–F distance in Figure 9. The total values are small and negative (between  $-2.8$  and  $-8.1$  Hz). The results present a clear lineal dependence ( $R^2 = 0.97$ ), increasing in absolute value with  $d(\text{F}-\text{F})$ , although the trend is opposite to the ones observed for  ${}^1J$  and  ${}^2J$ . This is the consequence of the compensation of a basically constant negative SO component (PSO + DSO) and the positive values due to the sum of the SD and FC contributions. The mentioned sum (SD + FC terms) shows also a good linear correlation with the  $d(\text{F}-\text{F})$  distance ( $R^2 = 0.95$ , Figure 10).

### 3.3.5. Intermolecular couplings between FCCF and $\text{H}_2\text{O}$

The calculated intermolecular coupling constants between FCCF and the  $\text{H}_2\text{O}$  molecules that show values larger than 1.0 Hz in absolute value correspond to F–H and F–O cases. They have been gathered in Table 6 and plotted in Figure 11.

When a direct interaction is observed between a fluorine atom and hydrogen, negative values of  ${}^1hJ(\text{H}-\text{F})$  are obtained, depicted with triangles in Figure 11. The coupling is stronger for the closest pair, as expected.

There are four non-negligible F–O couplings corresponding to tetrel bonds. For complexes **A** and **F**, these are clearly indicated in Figures 2 and 3. For complex **D**, each F nucleus is coupled to its closest O nucleus, the tetrel bond corresponding to the  $\text{H}_2\text{O}$  molecule with its H atoms pointing away from FCCF. For complex **E**, both F–O couplings are to the same F nucleus, the tetrel bond corresponding to the more distant O atom. The tetrel bond couplings are all negative, ranging between  $-8.4$  and  $-1.6$  and exhibiting a clear linear dependence with distance as depicted with squares in Figure 11.

The two remaining F–O couplings correspond to 2h bonds. They are small and positive, shown by circles in Figure 11.

## 4. Concluding remarks

In this work, we have systematically studied the changes in the inter- and intramolecular spin–spin coupled constants brought about by the presence of water molecules around difluoroacetylene [complexes  $\text{FCCF}:(\text{H}_2\text{O})_n$ ; with  $n = 1, 2$ ]. We have considered the three possible types

of bonds,  $\text{HOH}\cdots\pi$  interactions,  $\text{HOH}\cdots\text{FC}$  hydrogen bonds and  $\text{O}\cdots(\text{FC})$  tetrel bonds. We have also analysed the possible relation of the SSCCs to both the BP and BCP of the different compounds. We observe the following patterns.

The MEP of  $\text{C}_2\text{F}_2$  shows three distinct regions. Two negative ones, the fluorine ends and the  $\pi$  cloud, where the hydrogen atoms of  $\text{H}_2\text{O}$  could bind (complexes **C** and **B**, respectively), and a positive one, the C–F bonds, where the lone pairs of the oxygen atom of  $\text{H}_2\text{O}$  could interact via a tetrel bond (complex **A**).

The single bond critical point (BCP) in complexes **B** and **C**, and the two BCPs in complex **A** display characteristics typical of weak interactions.

Three unique minima have been located for  $\text{FCCF}:(\text{H}_2\text{O})_2$ . In all cases, the two  $\text{H}_2\text{O}$  molecules are mutually connected by an HB. All three complexes present an  $\text{O}\cdots\text{C}$  tetrel bond path, complemented by either an  $\text{H}\cdots\text{F}$  HB, an  $\text{O}\cdots\text{F}$  bond, or a pair  $\text{H}\cdots\pi$  HB plus  $\text{O}\cdots\text{F}$  tetrel bond.

All FCCF intramolecular couplings correlate linearly with the distance between the involved nuclei, except for  ${}^2J(\text{F}-\text{C})$  which instead depends linearly on the  $\text{C}\equiv\text{C}$  bond length as has previously been seen for corresponding complexes with HF.

All FCCF intramolecular couplings decrease in absolute value with distance, with the exception of  ${}^3J(\text{F}-\text{F})$ .

The  ${}^1J(\text{C}-\text{C})$  couplings range between 405 and 413 Hz and are completely dominated by the FC term. The  ${}^1J(\text{F}-\text{C})$  couplings are also large but negative in contradiction to the Dirac vector model, and in agreement with previous analyses that have reported similar discrepancies [6,61]. Their values range from  $-289$  to  $-256$  Hz, for bond lengths  $d(\text{F}-\text{C})$  that vary by  $0.15$  Å between complexes.

The  ${}^2J(\text{F}-\text{C})$  couplings are all positive, as are their three main contributions, PSO, SD and FC.

The  ${}^3J(\text{F}-\text{F})$  couplings are negative and exhibit the odd behaviour of a clearly linear increase in absolute value with the F–F distance.

Regarding intermolecular couplings, measurable results are predicted for  ${}^1hJ(\text{H}-\text{F})$  and  ${}^1hJ(\text{F}-\text{O})$ .

The only non-negligible intermolecular  ${}^1hJ(\text{H}-\text{F})$  coupling occur between hydrogen bonded pairs, and range from  $-4.4$  to  $-2.4$  Hz.

The intermolecular  ${}^1hJ(\text{F}-\text{O})$  couplings correspond to tetrel and 2h bonds. The former are negative, ranging between  $-8.4$  and  $-1.6$  and showing a linear decrease in absolute value with distance. The latter are positive and small, around 1 Hz.

## Disclosure statement

No potential conflict of interest was reported by the authors.

## Funding

MCC acknowledges financial support to the present research from CONICET [PIP0369] and Universidad de Buenos Aires [UBACYT,W197], IA acknowledges financial support from the Ministerio de Economía, Industria y Competitividad [Project No. CTQ2015-63997-C2-2-P] and Comunidad Autónoma de Madrid [S2013/MIT2841, Fotocarbon], P.F.P. acknowledges financial support from CONICET and UNNE [No. PI:15/F002 Res. 1017/15]; and SPAS thanks the Danish Center for Scientific Computing (DCSC) and the TWAS Visiting Expert Programmer [E.R. 3240301376] for financial support.

## ORCID

Ibon Alkorta  <http://orcid.org/0000-0001-6876-6211>

Stephan P. A. Sauer  <http://orcid.org/0000-0003-4812-0522>

## References

- [1] J.A. Pople, W.G. Schneider and H.J. Bernstein, *High-resolution Nuclear Magnetic Resonance* (McGraw-Hill, New York, 1959).
- [2] J.W. Emsley, J. Feeney and L.H. Sutcliffe, *High-resolution Nuclear Magnetic Resonance Spectroscopy* (Pergamon, Oxford, 1966).
- [3] R.H. Contreras, editor, *High Resolution NMR Spectroscopy: Understanding Molecules and their Electronic Structures* (Elsevier, Amsterdam, 2013).
- [4] K. Jackowski and M. Jaszunski, editors, *Gas Phase NMR, Royal Society of Chemistry* (Royal Society of Chemistry, London, 2016).
- [5] L.B. Krivdin and G.A. Kalabin, *Russ. Chem. Rev.* **57**, 1 (1988).
- [6] L.B. Krivdin and G.A. Kalabin, *Prog. NMR Spectrosc.* **21**, 293 (1989).
- [7] L.B. Krivdin and E.W. Della, *Prog. NMR Spectrosc.* **23**, 301 (1991).
- [8] L.B. Krivdin and S.V. Zinchenko, *Curr. Org. Chem.* **2**, 173 (1998).
- [9] R.H. Contreras, J.E. Peralta, C.G. Giribet, M.C. Ruiz de Azua and J.C. Facelli, *Ann. Rep. NMR Spectrosc.* **41**, 55 (2000).
- [10] L.B. Krivdin, *Prog. NMR Spectrosc.* **105**, 54 (2018).
- [11] N.F. Ramsey, *Phys. Rev.* **91**, 303 (1953).
- [12] J. Gräfenstein and D. Cremer, *Chem. Phys. Lett.* **383**, 332 (2004).
- [13] P.F. Provasi, M.C. Caputo, S.P.A. Sauer, I. Alkorta and J. Elguero, *Comput. Theoret. Chem.* **998**, 98 (2012).
- [14] H. Bürger and S. Sommer, *J. Chem. Soc. Chem. Commun.* **42**, 456 (1991).
- [15] J.E. Del Bene, P.F. Provasi, I. Alkorta and J. Elguero, *Magn. Res. Chem.* **46**, 1003 (2008).
- [16] H. Bürger, W. Schneider, S. Sommer, W. Thiel and H. Willner, *J. Chem. Phys.* **95**, 5660 (1991).
- [17] P.F. Provasi, G.A. Aucar and S.P.A. Sauer, *J. Phys. Chem. A* **108**, 5393 (2004).
- [18] M. Sanchez, P.F. Provasi, G.A. Aucar and S.P.A. Sauer, *Adv. Quantum Chem.* **48**, 161 (2005).
- [19] R. Faber and S.P.A. Sauer, *Phys. Chem. Chem. Phys.* **14**, 16440 (2012).
- [20] R. Faber, S.P.A. Sauer and J. Gauss, *J. Chem. Theory Comput.* **13**, 696 (2017).
- [21] R. Faber and S.P.A. Sauer, *Theor. Chem. Acc.* **137**, 303 (2018).
- [22] P.F. Provasi, G.A. Aucar, M. Sanchez, I. Alkorta, J. Elguero and S.P.A. Sauer, *J. Phys. Chem. A* **109**, 6555 (2005).
- [23] I. Alkorta, I. Rozas and J. Elguero, *J. Phys. Chem. A* **105**, 743 (2001).
- [24] A. Bauzá, T.J. Mooibroek and A. Frontera, *Angew. Chem., Int. Ed.* **52**, 12317 (2013).
- [25] J.R. Lane, J. Contreras Garcia, J.P. Piquemal, B.J. Miller and H.G. Kjaergaard, *J. Chem. Theory Comput.* **9**, 3263 (2013).
- [26] C. Møller and M.S. Plesset, *Phys. Rev.* **46**, 618 (1934).
- [27] M.J. Frisch, G.W. Trucks, H.B. Schlegel, G.E. Scuseria, M.A. Robb, J.R. Cheeseman, J.A. Montgomery Jr., T. Vreven, K.N. Kudin, J.C. Burant, J.M. Millam, S.S. Iyengar, J. Tomasi, V. Barone, B. Mennucci, M. Cossi, G. Scalmani, N. Rega, G.A. Petersson, H. Nakatsuji, M. Hada, M. Ehara, K. Toyota, R. Fukuda, J. Hasegawa, M. Ishida, T. Nakajima, Y. Honda, O. Kitao, H. Nakai, M. Klene, X. Li, J.E. Knox, H.P. Hratchian, J.B. Cross, V. Bakken, C. Adamo, J. Jaramillo, R. Gomperts, R.E. Stratmann, O. Yazyev, A.J. Austin, R. Cammi, C. Pomelli, J.W. Ochterski, P.Y. Ayala, K. Morokuma, G.A. Voth, P. Salvador, J.J. Dannenberg, V.G. Zakrzewski, S. Dapprich, A.D. Daniels, M.C. Strain, O. Farkas, D.K. Malick, A.D. Rabuck, K. Raghavachari, J.B. Foresman, J.V. Ortiz, Q. Cui, A.G. Baboul, S. Clifford, J. Cioslowski, B.B. Stefanov, G. Liu, A. Liashenko, P. Piskorz, I. Komaromi, R.L. Martin, D.J. Fox, T. Keith, M.A. Al-Laham, C.Y. Peng, A. Nanayakkara, M. Challacombe, P.M.W. Gill, B. Johnson, W. Chen, M.W. Wong, C. Gonzalez and J.A. Pople, *Gaussian 03, Revision C.02*, Gaussian, Inc., Wallingford, CT, 2004.
- [28] T.H. Dunning Jr., *J. Phys. Chem. A* **104**, 9062 (2000).
- [29] T. Helgaker, M. Jaszunski and K. Ruud, *Chem. Rev.* **99**, 293 (1999).
- [30] S.P.A. Sauer, *Molecular Electromagnetism: 'A Computational Chemistry Approach'* (Oxford University Press, Oxford, 2011).
- [31] L.B. Krivdin and R.H. Contreras, *Ann. Rep. NMR Spectrosc.* **61**, 133 (2007).
- [32] J. Vaara, *Phys. Chem. Chem. Phys.* **9**, 5399 (2007).
- [33] T. Helgaker, M. Jaszunski and M. Pecul, *Prog. Nucl. Magn. Reson. Spectrosc.* **53**, 249 (2008).
- [34] T. Helgaker, S. Coriani, P. Jørgensen, K. Kristensen, J. Olsen and K. Ruud, *Chem. Rev.* **112**, 543 (2012).
- [35] G.D. Purvis III and R.J. Bartlett, *J. Chem. Phys.* **76**, 1910 (1982).
- [36] G.E. Scuseria, A.C. Scheiner, T.J. Lee, J.E. Rice and H.F. Schaefer III, *J. Chem. Phys.* **86**, 2881 (1987).
- [37] J.F. Stanton, J. Gauss, J.D. Watts and R.J. Bartlett, *J. Chem. Phys.* **94**, 4334 (1991).
- [38] C. Hampel, K.A. Peterson and H.-J. Werner, *Chem. Phys. Lett.* **190**, 1 (1992).
- [39] H. Sekino and R.J. Bartlett, *J. Chem. Phys.* **85**, 3945 (1986).
- [40] S.A. Perera, H. Sekino and R.J. Bartlett, *J. Chem. Phys.* **101**, 2186 (1994).
- [41] S.A. Perera, M. Nooijen and R.J. Bartlett, *J. Chem. Phys.* **104**, 3290 (1996).
- [42] A.A. Auer and J. Gauss, *J. Chem. Phys.* **115**, 1619 (2001).
- [43] P. Provasi, G. Aucar and S.P.A. Sauer, *J. Chem. Phys.* **115**, 1324 (2001).
- [44] V. Barone, P.F. Provasi, J.E. Peralta, J.P. Snyder, S.P.A. Sauer and R.H. Contreras, *J. Phys. Chem. A* **107**, 4748 (2003).

- [45] CFOUR, a quantum chemical program package written by J.F. Stanton, J. Gauss, M.E. Harding, P.G. Szalay with contributions from A.A. Auer, R.J. Bartlett, U. Benedikt, C. Berger, D.E. Bernholdt, Y.J. Bomble, L. Cheng, O. Christiansen, M. Heckert, O. Heun, C. Huber, T.-C. Jagau, D. Jonsson, J. Jusélius, K. Klein, W.J. Lauderdale, D.A. Matthews, T. Metzroth, L.A. Mück, D.P. O'Neill, D.R. Price, E. Prochnow, C. Puzzarini, K. Ruud, F. Schiffmann, W. Schwalbach, S. Stopkowitz, A. Tajti, J. Vázquez, F. Wang, J.D. Watts and the integral packages MOLECULE (J. Almlöf and P.R. Taylor), PROPS (P.R. Taylor), ABACUS (T. Helgaker, H.J. Aa. Jensen, P. Jørgensen and J. Olsen), and ECP routines by A.V. Mitin and C. van Wüllen. For the current version, see <http://www.cfour.de>.
- [46] I.L. Rusakova and L.B. Krivdin, *Mendeleev Commun.* **28**, 1 (2018).
- [47] T.A. Ruden and K. Ruud, in *Calculation of NMR and EPR Parameters: Theory and Applications*, edited by M. Kaupp, V.G. Malkin and M. Bühl (Wiley-VCH, Weinheim, 2004), chap. 10, pp. 153–173.
- [48] R. Faber, J. Kaminsky and S.P.A. Sauer, in *Gas Phase NMR*, edited by K. Jackowski and M. Jaszunski (Royal Society of Chemistry, London, 2016), Chap. 7, pp. 219–268.
- [49] K. Ruud, L. Frediani, R. Cammi and B. Mennucci, *Int. J. Mol. Sci.* **4**, 119 (2003).
- [50] A. Møgelhøj, K. Aidas, K.V. Mikkelsen, S.P.A. Sauer and J. Kongsted, *J. Chem. Phys.* **130**, 134508 (2009).
- [51] K. Jackowski, W. Makulski, A. Szybowska, A. Antusek and M. Jaszunski, *Magn. Reson. Chem.* **47**, 857 (2009).
- [52] K. Sneskov and J.F. Stanton, *Mol. Phys.* **110**, 2321 (2012).
- [53] R. Faber and S.P.A. Sauer, *AIP Conf. Proc.* **1702**, 90035 (2015).
- [54] R.D. Wigglesworth, W.T. Raynes, S. Kirpekar, J. Oddershede and S.P.A. Sauer, *J. Chem. Phys.* **112**, 736 (2000).
- [55] R.D. Wigglesworth, W.T. Raynes, S. Kirpekar, J. Oddershede and S.P.A. Sauer, *J. Chem. Phys.* **112**, 3735–3746 (2000); R.D. Wigglesworth, W.T. Raynes, S. Kirpekar, J. Oddershede and S.P.A. Sauer, *J. Chem. Phys.* **114**, 9192 (2001).
- [56] A. Yachmenev, S.N. Yurchenko, I. Paidarová, P. Jensen, W. Thiel and S.P.A. Sauer, *J. Chem. Phys.* **132**, 114305 (2010).
- [57] T.A. Ruden, O.B. Lutnæs, T. Helgaker and K. Ruud, *J. Chem. Phys.* **118**, 9572 (2003).
- [58] O.B. Lutnæs, T.A. Ruden and T. Helgaker, *Magn. Reson. Chem.* **42**, S117 (2004).
- [59] S. Hirata, K. Yagi, S.A. Perera, S. Yamazaki and K. Hirao, *J. Chem. Phys.* **128**, 214305 (2008).
- [60] M. Pecul and K. Ruud, *Magn. Reson. Chem.* **42**, S128 (2004).
- [61] J.Cz. Dobrowolski, J.E. Rode and J. Sadlej, *Comp. Theor. Chem.* **964**, 148 (2011).
- [62] I. Alkorta and J. Elguero, *Struct. Chem.* **15**, 117 (2004).